Wood Science and Technology (2021) 55:659–679
https://doi.org/10.1007/s00226-021-01284-8

ORIGINAL

Comparative study on the conversion of *Acacia mangium* wood sawdust-derived xylose-containing acid hydrolysate to furfural by sulfonated solid catalysts prepared from different lignocellulosic biomass residues

Nguyen Hoang Chung[1] · Le Quang Dien[1] · Nguyen Thi Que[1] · Nguyen Trung Thanh[1] · Giang Thi Phuong Ly[1]

Received: 19 September 2020 / Accepted: 6 March 2021 / Published online: 24 March 2021

Abstract

This work focused on the thorough utilization of lignocellulosic biomass residues for the synthesis of carbonaceous sulfonated solid catalysts (CBSCs), which were then applied to the conversion of the same biomass source to furfural. Four different biomass materials were used, namely *Acacia mangium* wood sawdust, coconut shell (CS), sugarcane bagasse, and lignin-rich residue from an enzymatic saccharification of the wood sawdust. A facile multi-stage process for the preparation of CBSCs has been developed including impregnation, carbonization, and sulfonation at low temperature and long reaction time. Main characteristics of CBSCs including acidity, surface area, and surface morphology were analyzed through BET, EDS, TPD-NH_3, SEM, FTIR. CBSCs were applied to the conversion of acid hydrolysate of *Acacia mangium* wood sawdust to furfural for evaluation of catalytic activity. Influences of catalyst dosage on the xylose conversion, the furfural yield, and the furfural selectivity were evaluated based on the synthesis carried out at 150 °C for 7 h for comparison of the effectiveness of CBSCs. The highest yield of furfural was 28.6% when using CS-CBSC at the catalyst loading of 0.1 g/g. Furfural selectivity reached the best value of 70.8% when LR-CBSC was used at the dosage of 0.2 g/g.

Introduction

As the reserves of conventional fossil resources are rapidly descending, the use of lignocellulosic biomass, especially agricultural residues, has drawn much attention as this is an abundant renewable energy source that has not been used

✉ Le Quang Dien
dien.lequang@hust.edu.vn

[1] School of Chemical Engineering, Hanoi University of Science and Technology, 1. Dai Co Viet street, Hai Ba Trung Distric, Hanoi, Vietnam

thoroughly yet. Annually, great volumes of residues that have not been utilized completely are produced including rice straw, corncob, coconut shell, sugarcane bagasse and wood waste from paper industry. These materials are great sources of cellulose, hemicellulose, and lignin making them a promising lignocellulosic candidate for utilization. Recently, coconut shell was used as the raw material for production of activated carbon, which later showed good adsorption properties toward phenolic and furaldehyde groups (Freitas et al. 2019). Cocoa waste is another potential material that was able to be converted into biogas, biochar, and other valuable products via pyrolysis (Ghysels et al. 2020). Furthermore, the utilization of these materials will contribute significantly to the sustainable development of the country toward the UN's Sustainable Development Goals (SDG 2019).

Furfural is a key platform substance that can be used for further production of chemical building blocks, which are widely applied in chemical engineering and industry (Mariscal et al. 2016). According to the US Department of Energy (DOE), furfural is classified as one of the top 12 value-added products, with approx. 300,000 tons produced annually (Luo et al. 2019). China is the world's largest producer of furfural with a total production capacity of ~ 70%. Other furfural suppliers are Dominican Republic and South Africa (Mamman et al. 2008; Mariscal et al. 2016; Luo et al. 2019).

The synthesis of furfural is mainly carried out via hydrolysis and dehydration of xylose/pentose (Li et al. 2016), depolymerization and pyrolysis of cellulose (Zhang et al. 2014) or mannan-rich material (Ghysels et al. 2019a). The mechanism of furfural conversion from sugars and from biomass was reviewed in detail (Li et al. 2016). Among the three major components of lignocellulose, hemicellulose is a promising source for the production of furfural as xylan and pentosan are the main components of this material. Regarding the hydrolysis of biomass to form xylose/pentose, the use of sulfuric acid is still dominant (Danon et al. 2014; Žilnik et al. 2016; Delbecq et al. 2018), while solid acid catalysts are the most popular choice for the dehydration of xylose/pentose to form furfural (Li et al. 2014, 2017; Hara et al. 2015; Metkar et al. 2015; Bhaumik and Dhepe 2016; De et al. 2016; Zhang et al. 2017; Delbecq et al. 2018; Bayu et al. 2019; Luo et al. 2019). Generally, catalysts play an important role in hemicellulose conversion to furfural as they improve the efficiency, enhance the productivity, and reduce the cost of the process (Luo et al. 2019). Among a variety of heterogeneous catalysts, solid acid catalysts are well-known for many advantages over homogeneous catalysts such as easy separation and recovery, high catalytic activity making them great candidates for biomass conversion to furfural (Gromov et al. 2018).

Toward sustainable development goals, synthesis and application of biomass-derived carbonaceous sulfonated solid catalysts (CBSCs) for the conversion of lignocellulosic refineries to value-added products have been drawing much attention. Unlike conventional solid acids, CBSCs possess three acidic groups, namely $–SO_3H$, –COOH, and phenolic –OH making them more flexible with many applications (Suganuma et al. 2008; Wang et al. 2011; Kang et al. 2013b; Lin et al. 2019). On the one hand, $–SO_3H$ and –COOH groups act as Brønsted acids that contribute mainly to the active acidic sites of the catalysts. On the other hand, –COOH and

phenolic –OH are hydrophilic groups that provide the catalysts better contact and more effective reaction with water and reactants (Kang et al. 2013b).

The preparation of CBSCs from various carbon-based raw materials including biomass has been summarized and reviewed thoroughly by Kang et al. (2013b). CBSCs are mainly synthesized by carbonization and sulfonation. Firstly, biochar is produced by carbonization of biomass at a temperature ranging from 265 to 650 °C using concentrated sulfuric acid. Secondly, it is recommended to carry out the sulfonation of the biochar at low temperature (below 100 °C) and longer time to obtain CBSCs with high catalytic activity. Concentrated sulfuric acid is widely used in this preparation procedure. To improve surface area of the final catalyst, it is necessary to activate the biochar before it is sulfonated. In this work, an impregnation process was conducted with the biomass using concentrated phosphoric acid. This procedure aims to activate the material for better carbonization and to produce CBSCs with high catalytic activity later.

Acacia mangium and *Eucalyptus urophilla* are two main feedstocks for the paper industry in Vietnam and other Asian countries. With over 8 million tons of wood chips produced per year, Vietnam was one of the largest wood chips exporters in the world (VPPA 2019). As a consequence, wood sawdust—a residue of the wood chip production—is available in large quantities (about 2% of the wood chips), which can be utilized for the production of many value-added products. As an agricultural country, Vietnam also has many other agricultural residues that can become promising sources of biomass, including coconut shell, rice straw, corncob, and sugarcane bagasse.

This work aimed at the preparation and characterization of CBSCs from four different sources of lignocellulose, including *Acacia mangium* wood sawdust, coconut shell, sugarcane bagasse and lignin-rich residue. The catalysts were then applied to the production of furfural (also 5-HMF) from the wood sawdust. Catalytic activity of the synthesized catalysts was evaluated and compared to each other based on xylose conversion, furfural yield, and furfural selectivity. This work will provide a new point of view on the utilization of some renewable carbon-based materials for the production of solid acid catalysts. This can significantly contribute to the sustainable production of value-added products from Vietnam's paper industry.

Materials and methods

Materials

Cellulase Cellic Ctec2 (SAE0020) with activity of 874 FPU/g, a commercial enzyme blend was purchased from Sigma-Aldrich. Other analytical chemicals were also supplied by Sigma-Aldrich including H_2SO_4 (aqueous solution, concentration of 95 wt%), H_3PO_4 (aqueous solutions, concentration of 85 wt%), NaOH (solid, purity of 97%), glucose (powder, HPLC grade, purity of 99.5%), xylose (powder, HPLC grade, purity of 99.0%), and furfural (powder, purity of 99%).

Acacia mangium wood sawdust (WS) was supplied by Bai Bang paper mill. Coconut shells (CS)—residue of the coconut processing—was collected from Ben

Tre province, the "capital" of coconuts in Vietnam. Sugarcane bagasse (SB) was collected from Lam Son sugar Company (Thanh Hoa, Vietnam). These lignocellulosic materials were air-dried and then ground to a suitable size of 1–5 mm. The materials were then stored in closed plastic bags at room temperature for further experiments and investigations. Major biochemical constituents of the lignocellulosic materials, including cellulose, lignin, pentosan, and ash content were determined according to TAPPI methods number T17 wd-70, T222, T223, and T211 om-93, respectively.

Lignin-rich residue was obtained from the three-step treatment of the *Acacia mangium* wood sawdust mentioned above (as shown in Fig. 1). The WS was first hydrolyzed with dilute sulfuric acid, followed by an alkaline pulping process. The obtained cellulose pulp was then subjected to an enzymatic saccharification with cellulase SAE0020 to convert cellulose into glucose. The residue, which was rich

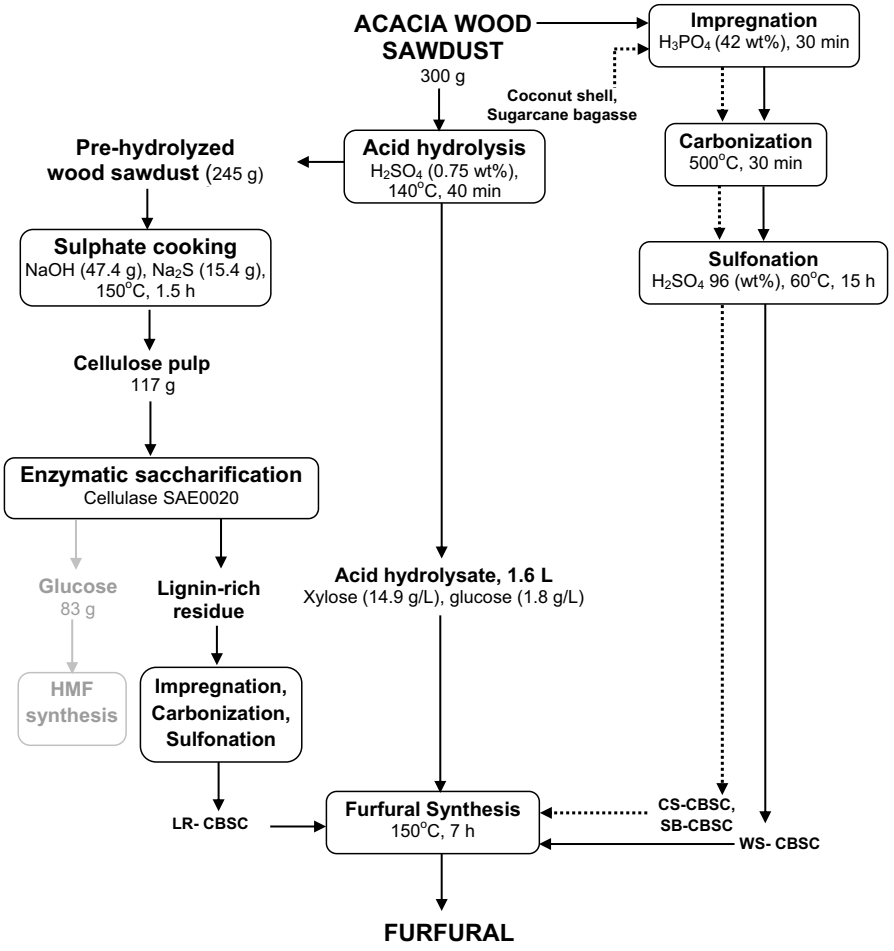

Fig. 1 Schematic representation of integrated preparation of carbonaceous solid acid catalyst, 5-hydroxymethylfurfural and furfural

in lignin, was collected, washed, and stored as the fourth object in this study. The obtained glucose was used for the synthesis of 5-hydroxymethylfurfural in another work.

Preparation and characterization of carbonaceous solid acid catalyst

The porous carbonaceous solid acid catalysts (CBSCs) were prepared following the method described by Thanh et al. (2019). According to this method, approx. 20 g of the lignocellulosic biomass was first impregnated with 42 wt% phosphoric acid solution at the solid-to-liquid ratio of 1–3. The impregnation was conducted in a 150-mL autoclave at 50 °C for 30 min. Subsequently, the autoclave was placed in an oven, which was previously set at 500 °C, and maintained at this temperature for 40 min to obtain porous biochar. The biochar was separated from the liquid part and washed with hot water until the washing water became neutral. It was finally dried at 105 ± 2 °C for 180 min to reach the activated state. In the second stage, the activated porous biochar was treated with 96 wt% sulfuric acid (5 mL of sulfuric acid per 1 g of the biochar) in a Teflon lined autoclave reactor at 60 °C for 16 h. The sulfonated biochar was then thoroughly washed with hot water until the washing water became neutral, dewatered and dried at $105 \pm 2°$ for 180 min. Finally, the product was ground to fine powder form of CBSC. Each experiment was run in duplicate.

Typical structural properties of the products, including surface area, pore structure, particle size of the catalyst, were characterized via Brunauer–Emmett–Teller (BET), scanning electron microscopy (SEM), and Fourier-transform infrared spectroscopy (FTIR) techniques.

Specific surface area and pore size distribution of the biochar and catalysts were calculated via N_2 sorption/desorption isotherm, carried out on a BET Micrometrics Gemini VII instrument. Samples were degassed for removing air and moisture at different temperatures, from room temperature (about 30 °C) up to 300 °C with weight determination. Subsequently, they were immersed in liquid nitrogen (-196 °C) for adsorption. Surface area was calculated using Brunauer–Emmett–Teller (BET) equation. Pore size distributions were determined using the Barrett-Joyner-Halenda (BJH) method.

Structural morphology of the carbon materials was investigated with a JEOL JSM-7600F scanning electron microscope (SEM). The samples of carbon material were refined and then placed lengthwise onto a copper bar with the ends secured by press-on silver glue tabs. High-resolution images of the samples were recorded at different locations along the fiber length at an acceleration potential of 10.0 kV with magnification ranging from 1000 to 3000 times.

Elemental analysis was conducted with a field emission scanning electron microscope (FE-SEM) integrated with energy-dispersive X-ray spectroscopy (EDS) and equipped with a Gatan MonoCL4 Cathodoluminescence Detector (CL) on a JEOL JSM-7600F (USA). EDS analyses were performed using a 500 mm^2 X-Max EDS Silicon Drift Detector 5000 with an operating voltage of 15 keV and a working distance of 39 mm.

Acidity of the CBSCs, which is reflected by the amount and strength of acid sites, was measured by temperature-programmed desorption of ammonia (NH_3-TPD) on an AutoChem II 2920 instrument, degassed with helium at 90–110 °C. Temperature was programmed from 150 to 900 °C, with heating rate of 10 °C/ min. The desorption of NH_3 was recorded with a thermal conductivity detector. The stronger the acid sites, the stronger sorption of NH_3 molecules, and the higher desorption temperature. Acid site density of the catalysts was calculated according to 1–1 principle (i.e., one acid site adsorbs 1 ammonia molecule).

Structure of the samples was also characterized via their Fourier-transform infrared (FTIR) spectra, which were recorded with a SHIMADZU FITR 1S Fourier-transform infrared spectrometer using KBr pellet method. The samples were ground with potassium bromide (KBr) and pressed to form transparent round sheets. Water and moisture should be eliminated to avoid noise in the measurement.

Acid hydrolysis of wood sawdust

The experimental scheme of this work is summarized and presented in Fig. 1.

The hydrolysis was carried out under the optimal conditions described by Chung et al. (2019). Three hundred grams (o.d.) of *Acacia mangium* wood sawdust was placed in a 5-L reactor. Subsequently, 0.75 wt% sulfuric acid solution was added to reach the solid-to-liquid ratio of 1:8. The reactor was heated from 30 to 140 °C within 25 min. The system was maintained at the desired temperature for 40 min. After the reaction time, ~ 1.6 L of the hydrolysate, which mainly contained reducing sugars, was separated from the solid residue by filtration. The hydrolysate was used for the synthesis of furfural. The residue was thoroughly washed, dried, and stored for further characterizations followed by an enzymatic saccharification.

Furfural synthesis

The synthesis was conducted according to the method described by Thanh et al. (2019). Each experiment was carried out in a 500-mL Parr stirred reactor in which 150 mL of the acidic hydrolysate and a certain amount of CBSCs were added. The reaction was conducted at 150 °C and approx. 2.0 atm for 7 h. Furfural produced in vapor form was continuously collected via a condenser that was connected to the reactor. The condensation was supported with cooling water (around 8 °C) generated by using a 22 L JSR refrigerated circulation bath.

As the product was evaporated during the reaction, the liquid level in the flask was maintained by adding water regularly. Control experiments were carried out in the same way apart from the addition of the CBSCs. In all experiments, two replications were conducted for each reaction.

Alkali treatment and enzymatic saccharification of wood sawdust

The hydrolyzed WS, which was obtained from the acid hydrolysis described above was subject to an alkali treatment (i.e. sulfate pulping) (Thanh et al. 2019). The material

was treated with a mixture of sodium hydroxide and sodium hydrosulfite in a 5-L reactor at 150 °C for 1.5 h. The solid-to-liquid ratio was 1:4; active alkali charge was 25% over the o.d. weight of WS; sulfidity was 25%. After the treatment, the pulp was separated from the black liquor, neutralized with acetic acid, and washed with de-ionized water for several times before it was enzymatically saccharified. Moisture content of the pulp and pulping yield were also determined.

The enzymatic saccharification was carried out at 50 °C for 120 h in a 500-mL flask at the solid-to-liquid ratio of 1:10. Sodium citrate solution (0.05 M, pH ~ 5.2) was used as a buffer, and enzyme dosage over the o.d. mass of the pulp was 350 FPU/100 g. After the hydrolysis, the hydrolysate was separated from the solid residue and used for the conversion into HMF. The lignin-rich residue (LR) was washed with water for several times, dried, and used for the preparation of LR-CBSC.

Analysis and characterization of sugars and furfural

Glucose and xylose contents of sugar-containing solutions were analyzed using an Agilent 1200 HPLC, which was equipped with a Prevail™ Carbohydrate ES-GRACE 250×4.6 mm column and a RID G1362A Agilent 1200 detector. Temperature of the column was set at 40 °C during the analysis. The mobile phase was non-deionized water/acetonitrile (30/70 v/v) and its flow rate was set at 1.5 mL/min. For the determination of furfural, an Agilent Eclipse XDB-C18 column, together with an Ultraviolet Detector at 265 nm were installed. The mobile phase in this case was methanol/water (20/80 v/v) and the flow rate was set at 1.2 mL/min.

All tests were run in triplicates with significant differences of less than 1.5%. Xylose conversion or furfural yield was calculated based on the reacted amount of xylose or the total amount of furfural formed over the initial amount of xylose as shown in Eqs. (1) and (2).

$$\text{Xylose conversion}(\%) = \frac{\text{Reacted amount of xylose(mole)}}{\text{Initial amount of xylose(mole)}} \times 100 \quad (1)$$

$$\text{Furfural yield}(\%) = \frac{\text{Total amount of furfural formed(mole)}}{\text{Initial amount of xylose(mole)}} \times 100 \quad (2)$$

Noticeably, the total amount of furfural included a small part of furfural that was trapped in the reaction medium and could not be distilled. This part of furfural was able to be decomposed when the reaction time was extended. Therefore, furfural selectivity was introduced as the third parameter to be concerned and was determined according to Eq. (3).

$$\text{Furfural selectivity}\ (\%) = \frac{\text{Formed amount of furfural (mole)}}{\text{Reacted amount of xylose (mole)}} \times 100 \quad (3)$$

Results and discussion

Biochemical constituents of the lignocellulosic materials

The major biochemical constituents of the four biomass materials are presented in Table 1. The wood sawdust (WS), which contained a significant amount of wood bark, was partly decomposed to water-soluble substances due to long time storage. Therefore, the pentosan content of WS is usually lower than other lignocellulosic materials. Therefore, the composition of other substances in WS, which was not possible to identify, is quite high with 22.28%. Coconut shell contains high amount of lignin and pentosan, which is reflected by the naturally hard (high-density) structure of this material. Lignin-rich residue was the part that remained after the enzymatic hydrolysis of the WS derived cellulose pulp. Among the four materials, LR contained the highest content of cellulose with 57.38%, which could be because cellulose in pulp was not totally decomposed, while lignin and pentosan were not hydrolyzed during this reaction. As a representative of typical annual plants, sugarcane bagasse contains higher percentage of ash (i.e., 5.19%) and lower content of lignin and pentosan when compared to WS. In general, these lignocellulosic materials have relatively high amount of lignin, making them suitable candidates for the production of solid acid catalysts.

The data confirm that these are potential materials for the production of many value-added products, especially for the synthesis of furfural and sulfonated carbonaceous catalysts as stated in the aim of this work.

The alkali treatment of *Acacia mangium* wood sawdust carried out by the method mentioned above (section Alkali treatment and enzymatic saccharification of wood sawdust, Fig. 1) results in cellulose pulp with a yield of 28.17 wt% over oven-dry weight of the raw material. The cellulose pulp containing 78.64% of cellulose, 4.25% of lignin, 11.37% of pentosan, and 0.27% of ash was then subjected to the enzymatic saccharification as described in section Alkali treatment and enzymatic saccharification of wood sawdust.

Table 1 Chemical compound of biomass residues

Component	Content (%)				Analytical method
	Wood sawdust	Coconut shell	Lignin-rich residue	Sugarcane Bagasse	
Cellulose	40.94	31.87	57.38	44.02	TAPPI T17 wd-70
Lignin	21.16	37.42	29.52	25.49	TAPPI T222
Pentosan	14.98	28.74	10.11	18.71	TAPPI T223
Ash	0.64	0.58	2.36	5.19	TAPPI T211 om-93
Others	22.28	1.39	0.63	6.59	–

Structural characterization of the CBSCs

As mentioned earlier, the preparation of CBSCs consisted of three stages: impregnation (i.e., activation of carbon), carbonization, and sulfonation. Table 2 summarizes some characteristics of the lignocellulosic materials after each step of the treatment.

The yields of the activated carbon materials obtained from WS, LR, CS and SB were 32.6%, 28.2%, 35.2%, and 31.7%, respectively. According to Table 2, the activated carbon from coconut shell (CS-AC) has the highest C content with 83.87%. The lowest C content (63.42%) belongs to the activated carbon material from lignin-rich residue (LR-AC), but this material contains the highest percentage of oxygen element. This may correlate with the lignin content of the materials as shown in Table 1 as C content relates to the lignin composition. The same relation is found between O content and the total carbohydrates (i.e., cellulose and hemicellulose). According to Table 1, LR has a total amount of cellulose and hemicellulose of 67.49%, which is significantly higher than those of CS (60.61%) and of WS (55.92%). The WS-AC prepared in this work has similar C content but lower amount of O when compared to the non-activated carbon produced from *Leucocephala glauca* wood sawdust at 500 °C for 1 h (Pituya et al. 2017), whereas C composition of the LR-AC is close to the biochar from lignin-rich digested stillage of bioethanol production (63.42% vs. 50–66%) (Ghysels et al. 2019b). In comparison with the non-activated carbon from coconut shell fabricated by Pituya et al. (2017), the percentage of carbon in the LR-AC is significantly higher (83.87% vs. 64–65%).

Table 2 Acidity, element and pore analysis of CBSCs

Samples	Total acid density (mmol/g)	Element analysis (%)				Surface area (m^2/g)	Pore volume (cm^3/g)	Pore size (Å)
		C	O	S	P			
Non-activated carbonized materials (NAC)								
WS-NAC	–	–	–	–	–	1.91	0.018	533.182
LR-NAC	–	–	–	–	–	16.92	0.064	367.370
CS-NAC	–	–	–	–	–	140.13	0.019	74.879
SB-NAC	–	–	–	–	–	3.05	0.701	437.869
Activated carbonized materials (AC)								
WS-AC	–	77.31	12.61	0.11	–	793.67	0.293	27.561
LR-AC	–	63.42	30.23	0.32	1.17	657.06	0.050	145.011
CS-AC	–	83.87	15.01	0.22	0.06	307.92	0.109	31.790
SB-AC	–	77.95	21.46	0.06	0.00	574.24	0.223	27.416
Carbon-based sulfonated catalysts (CBSC)								
WS-CBSC	4.70	78.20	7.50	2.30	-	937.43	0.714	36.097
LR-CBSC	7.22	86.85	10.94	1.55	0.72	729.46	0.179	42.290
CS-CBSC	6.15	90.26	6.34	1.91	0.76	508.03	0.123	32.411
SB-CBSC	10.65	66.68	29.42	3.21	0.02	503.95	0.334	26.229

WS Wood sawdust, *LR* Lignin-rich residue, *CS* Coconut shell, *SB* Sugarcane bagasse, *CBSC* carbonized sulfonated catalyst

As can be seen from Table 2, WS-AC, LR-AC, CS-AC, and SB-AC contain relatively low contents of S with 0.11, 0.32, 0.22, and 0.06%, respectively. After the sulfonation, the S contents of these materials reach their corresponding values of 2.30, 1.55, 1.91, and 3.21%. This indicates that the sulfonation successfully attached $-SO_3H$ groups onto the activated carbon materials to create carbon-based sulfonated catalysts.

Regarding the surface properties of the activated carbon materials, the specific surface areas of WS after the carbonization increases dramatically from 1.91 to 793.67 m^2/g (i.e., over 400 times). The value of this parameter also increases slightly in the case of CS (from 140.13 to 307.92 m^2/g). However, the surface area of LR-AC almost remains unchanged (16.92 m^2/g vs. 15.06 m^2/g). Obviously, the structure of raw materials, reaction temperature and time, and acid used for the activation step have strong influences on the structural properties and the catalytic activity of the products (Tomczyk et al. 2020). The literature related to the synthesis of lignin-derived solid acids also confirmed the key role of acid in the impregnation (Zhu et al. 2019). When using sulfuric acid in the activation step, the obtained sulfonated solid acids possessed low surface area and porosity but showed excellent catalytic performance in esterification, hydrolysis, and dehydration. On the other hand, using phosphoric acid in the activation of lignin resulted in lignin-derived solid acids with well-developed porous structure, great thermal stability and excellent catalytic activity in dehydration.

In comparison with LR, WS, SB, and CS possess porous structure in their cell walls and also have more functional groups, which are decomposed during the multi-stage treatment process. In addition, phosphoric acid is penetrated into the materials during the impregnation leading to pores expansion and structural changes (Liu et al. 2015). As a result, more and more pores are formed during the pyrolysis.

Porosity of the materials is also reflected through pore volume and pore size (data presented in Table 2) as well as their surface morphology as shown in Fig. 2. The partially destroyed carbonized capillaries of wood cell walls are visible on the SEM images of WS-CBSC. The particles of LR-CBSC have the form of carbonized fibrils, which indicates the presence of cellulose and hemicellulose fibrils in the lignin-rich residue. Narrow capillaries are also observed in the SEM image of CS-CBSC.

As it can be observed in Table 2, all of the non-activated carbonized materials have small pore volume and large pore size. After the carbonization, WS-AC has the smallest pore size (27.561 Å) and the largest surface area (793.67 m^2/g). In addition, the SB-AC also has a small pore size of ~ 27.41 Å. This is apparently related to the typical structure of hardwood and bagasse cell wall. In the lignin-rich residue, the cell wall no longer exists, capillary structure is destructed, while its density is still high. As a result, the pore size of LR-AC is much larger than that of CS-AC (145.01 vs. 31.790 Å), but the pore volume is the smallest (0.050 cm^3/g) when compared to the other two materials. This indicates that the structure of raw material is not responsible for the formation of the porous structure, but the space created among the components of the lignocellulosic materials after the carbonization.

According to the pore data shown in Table 2, all of the non-activated carbon materials possess low surface areas (ranging from 1.91—140.13 m^2/g) with medium and

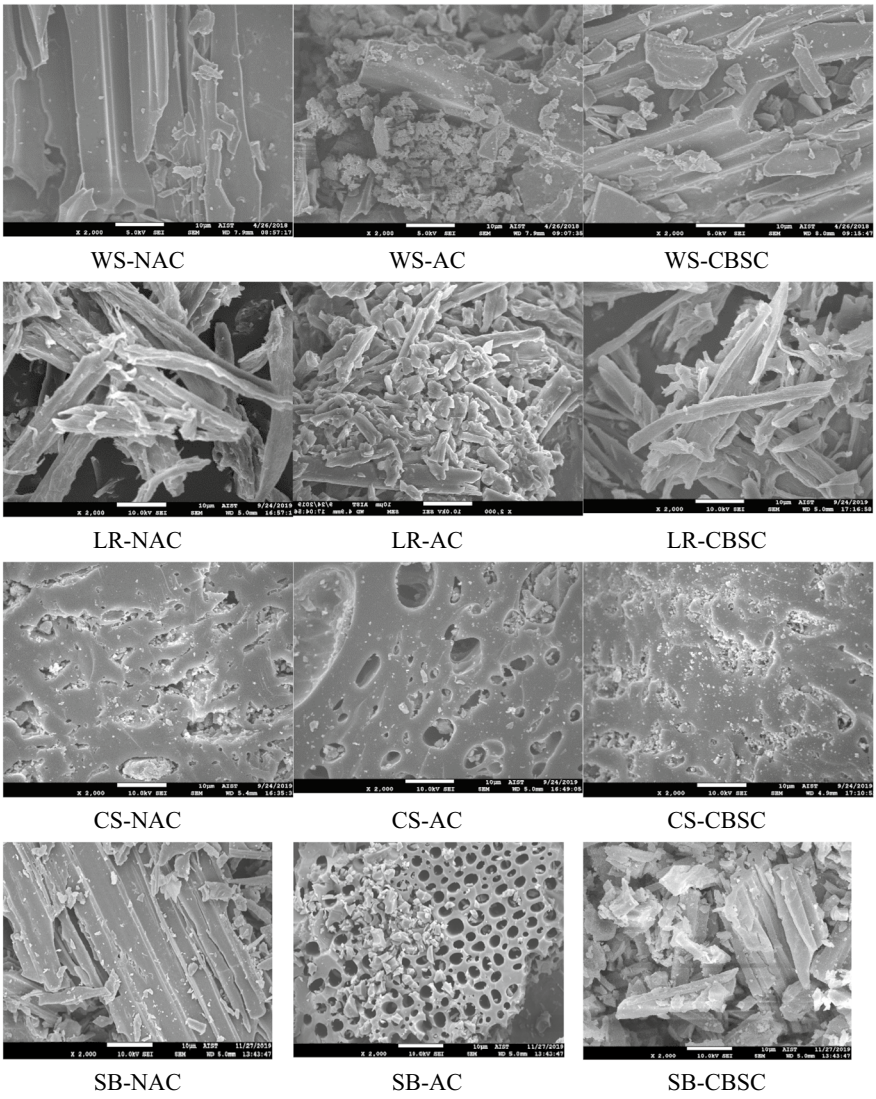

Fig.2 Surface morphology of carbonized materials and sulfonated catalysts (*NAC* Nonactivated carbonized material, *AC* Activated carbonized material, *CBSC* carbonized sulfonated catalyst, *WS* Wood sawdust, *LR* Lignin-rich residue, *CS* Coconut shell, *SB* Sugarcane bagasse)

large pores resulting in low pore volumes (ranging from 0.018–0.701 cm^3/g). After the activation with phosphoric acid, the specific areas of these materials increase dramatically with the appearance of medium pores. The average pore size of LR-AC was 145.01 Å, while that of SB-AC, WS-AC, and CS-AC ranged from 27–32 Å. A lower total pore volume of LR-AC compared to the other samples indicates that fewer pores were created in LR-AC after the activation. This is in an agreement with

the structure of the raw materials. WS-AC, SB-AC, and CS-AC were produced from the materials that had cell wall structure (which can be observed from SEM images of WS-NAC, SB-NAC, CS-NAC in Fig. 2), while the cell wall structure no longer existed in LR-NAC. The presence of pores inside the materials with cell wall structure allows activation agents like phosphoric acid easily penetrate and absorb. The structure without cell walls of LR-NAC makes it harder for H_3PO_4 to break into the material, resulting in fewer pores and lower pore volume compared to the others.

The surface area of the activated carbonized materials is improved after the sulfonation. In the case of LR-AC, this parameter increases from 657.06 to 729.46 m^2/g. With WS-AC and CS-AC, the surface area slightly ascends from 793.67 to 937.43 m^2/g and from 307.92 to 508.03 m^2/g, respectively. After the sulfonation, there is almost no change in pore size of the CBSCs obtained correspondingly from the CS-AC and SB-AC (~ 31.790 vs. 32.411 Å and ~ 27.416 vs. 26.229 Å, respectively). These pore sizes are in mesopore range. However, the pore size of LR-CBSC reduces noticeably from 145.011 to 92.290 Å.

LR-CBSC and CS-CBSC have nearly similar C content and slightly higher than the one in WS-CBSC. Trace amounts of phosphorous are found in LR- and CS-CBSC (0.72–0.76%), while it cannot be detected in WS-CBSC samples. This suggests that the remaining phosphorous elements might be adsorbed by the carbonized materials mentioned above.

Acidity is another important property of CBSCs. Under the same conditions of fabrication, the synthesized catalysts are arranged in descending order of acidity as follows: SB-CBSC > LR-CBSC > CS-CBSC > WS-CBSC. The sugarcane bagasse shows better potential for the synthesis of CBSC as it possesses the highest acidity with 10.65 mmol/g. The lowest acidity belongs to WS-CBSC with 4.70 mmol/g. Compared with the literature, the total acidities of the CBSCs synthesized from wood sawdust, coconut shell, and alkaline lignin were 2.57 mmol/g (Liu et al. 2013b), 3.18 mmol/g (Endut et al. 2017), and 2.56 mmol/g (Zhu et al. 2017), respectively. It is noticeable that the CBSCs obtained in this work have higher acidities. BET data also show that specific surface area of the current catalysts is also higher than that of metal modified zeolites, which can also be used for the synthesis of furfural from biomass-derived carbohydrates (Zhang et al. 2017). Large surface area and lengthening of the sulfonation at low temperature could be the reason behind this.

The profile of TPD-NH_3 presented in Table 3 and Fig. 3 clearly shows the presence of acid sites and their density. Higher desorption temperature of acid sites indicates stronger acidity of the corresponding acidic functional groups (Marikutsa et al. 2018). At temperatures lower than 250 °C, weak acid sites exist, while at higher temperature regions, i.e., 300–500 °C, 500–800 °C, and above 800 °C, there are mostly strong, very strong, and super strong acid sites, respectively. Acid sites appearing at the temperature of 300 °C and above represent -SO_3H groups formed after the sulfonation of the AC materials (Liu et al. 2013a). LR-CBSC contains weak, strong, very strong, and super strong acid sites while there are no strong acid sites in CS-CBSC and no super strong acid sites in WS-CBSC. The total amount of very strong and super strong acid sites in CS-CBSC is slightly higher than that in LR-CBSC (i.e., 5.89 mmol/g vs. 5.74 mmol/g). Among the

Table 3 Ammonia temperature programmed desorption (TPD-NH_3) analysis of CBSCs

Catalysts	Peak number	Maximum temperature (°C)	Quantity of acid sites (mmol/g)	Strength of acid sites[1]
WS-CBSC	1	157.0	0.24	w
	2	497.7	1.26	s
	3	611.3	3.20	vs
CS-CBSC	1	206.9	0.26	w
	2	675.3	3.20	vs
	3	814.6	1.04	ss
	4	899.0	1.65	ss
LR-CBSC	1	193.9	0.27	w
	2	480.1	1.21	s
	3	608.1	4.77	vs
	4	892.0	0.97	ss
SB-CBSC	1	170.0	0.28	w
	2	386.9	1.29	s
	3	526.6	8.45	vs
	4	897.6	0.63	ss

[1]*w* weak, *s* strong, *vs* very strong, *ss* super strong

WS Wood sawdust, *LR* Lignin-rich residue, *CS* Coconut shell, *SB* Sugarcane bagasse, *CBSC* carbonized sulfonated catalyst)

four catalysts that were synthesized in this work, WS-CBSC does not have super strong acid sites, while super strong acid sites are available in CS-CBSC, LR-CBSC, and SB-CBSC with total quantity of 2.69, 0.97, and 0.63 mmol/g, respectively. Especially, CS-CBSC has much more super strong acid sites (2.69 mmol/g, desorption temperature of 800 °C) than LR-CBSC (0.97 mmol/g). In the case of the SB-CBSC, although the total amount of acid sites is higher than the CS-CBSC, the total amount of super strong acid sites is lower. This indicates that CS-CBSC can be considered to have better potential among the four candidates for the application to chemical conversions.

The presence of functional groups in the fabricated catalysts is confirmed by FTIR spectra of the materials at all stages of the synthesis as shown in Fig. 4. A peak at the wavelength of around 3348 cm^{-1} observed in all cases indicates stretching vibrations of –OH groups in –COOH or phenolic compounds that are generated during the carbonization and sulfonation (Hu et al. 2013, 2015). The bands at around 1170 and 1033 cm^{-1} in the spectra of CBSCs are, respectively, assigned to asymmetric and symmetric stretching vibrations of O=S=O bonds in $–SO_3H$ groups (Chen and Fang 2011). This indicates that $-SO_3H$ groups are successfully attached to the activated carbonized materials via sulfonation. In addition, a peak at around 1699 cm^{-1} is allocated to stretching vibration of C=O bonds (Kang et al. 2013a; Lin et al. 2019). The existence of –OH and –COOH groups in CBSCs provides hydrophilic reactants the possibility to access $-SO_3H$ groups. In addition, the high acidity of these groups also leads to the effective catalytic performance of the CBSCs.

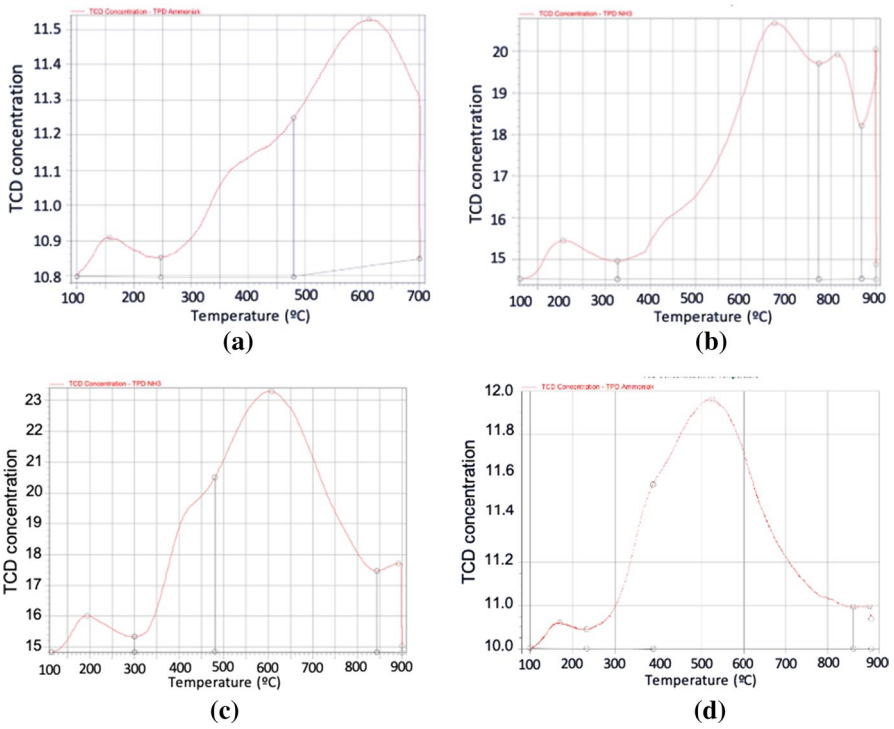

Fig. 3 TPD ammonia analysis of WS-CBSC catalyst **a**, CS-CBSC catalyst **b**, LR-CBSC catalyst **c**, and SB-CBSC catalyst **d**

Evaluation of the furfural synthesis using different CBSCs

The hydrolysate collected after the acid hydrolysis was used for the synthesis of furfural. The reaction is catalyzed by the achieved CBSCs as described earlier in Fig. 1 and section Furfural synthesis. According to HPLC data, the hydrolysate mainly contains xylose and glucose with contents of 14.96 and 1.81 g/L, respectively. In the following subsections, the influences of catalyst loading on the sugar conversion, furfural yield, and furfural selectivity were investigated. Reaction temperature and time were set, respectively, at 150 °C and 7 h for all experiments in this section. The three CBSCs were used at dosages of 0.1–1.0 g of catalyst/g of xylose in the hydrolysate.

Influences of catalyst loading on the xylose conversion

Figure 5 shows the xylose conversion in percentage corresponding to CBSCs and catalyst dosages used. Increasing catalyst loading from 0.1 to 1.0 g/g leads to significant improvement in the xylose conversion for all of the three CBSCs.

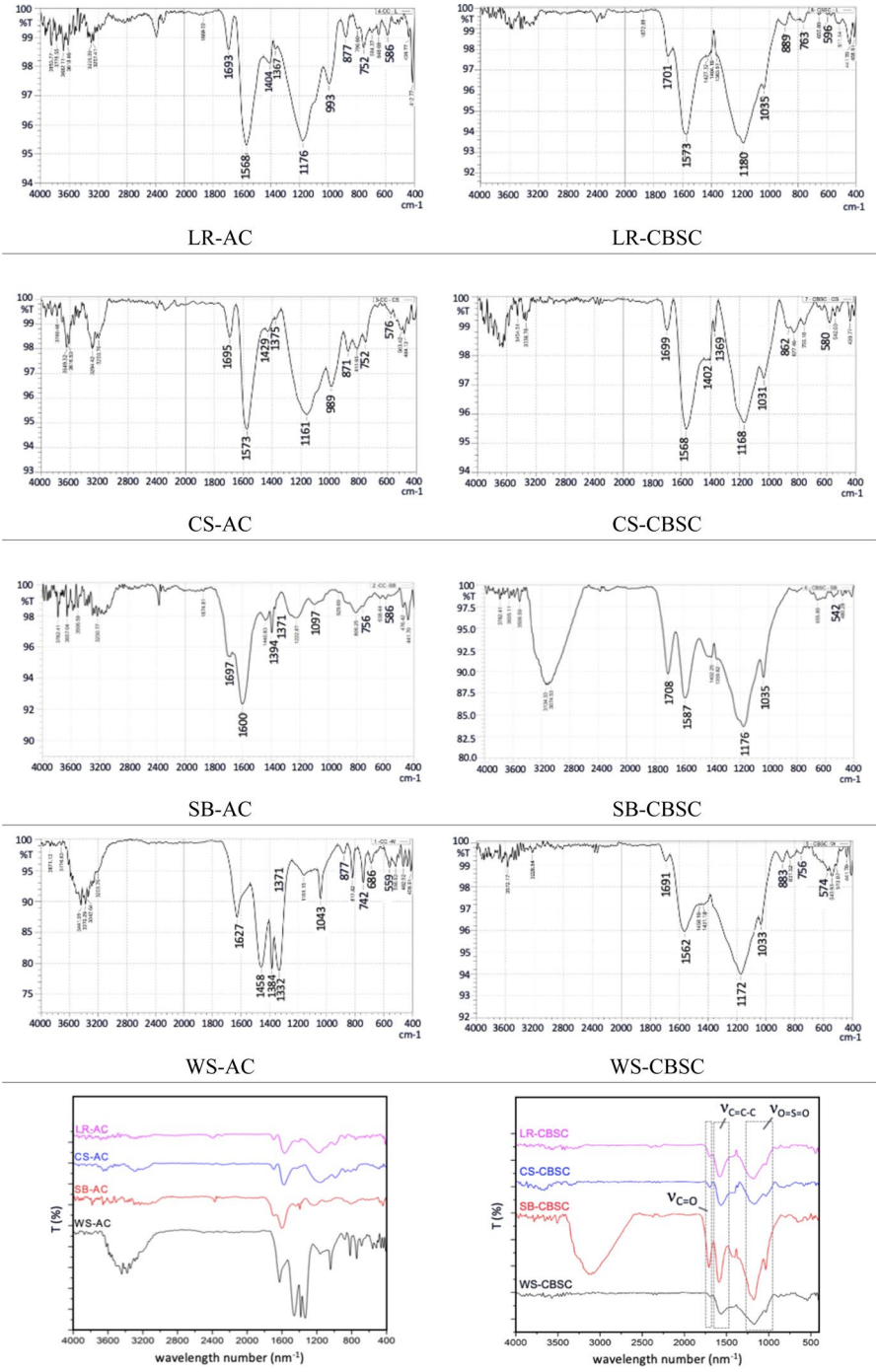

Fig. 4 FTIR spectra of biomass-derived activated carbon materials and sulfonated catalysts (*AC* Activated carbonized material, *CBSC* carbonized sulfonated catalyst, *WS* Wood sawdust, *LR* Lignin-rich residue, *CS* Coconut shell, *SB* Sugarcane bagasse)

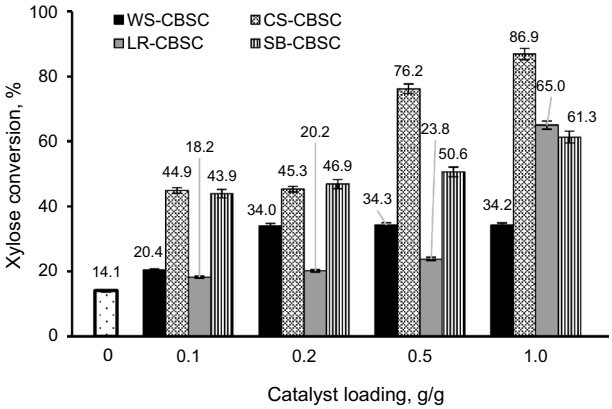

Fig. 5 Influence of catalyst loading on xylose conversion; reaction conditions: temperature 150 °C, time 7 h (*WS Acacia mangium* wood sawdust, *LR* lignin-rich residue, *CS* coconut shell, *SB* sugarcane bagasse, *CBSC* carbonaceous sulfonated solid acid catalyst)

However, each CBSC shows a different trend of changes. The conversion of xylose when WS-CBSC is used seems to be limited as this parameter increases slightly from 20.4 to 34.0% (corresponding to catalyst doses from 0.1 to 0.2 g/g). Higher dose of WS-CBSC does not make any significant change in the xylose conversion as it stays at around 34.2–34.3%. At any catalyst doses used, CS-CBSC always shows its best efficiency in the conversion of xylose. The xylose volume is dramatically enhanced when the amount of CS-CBSC or LR-CBSC is increased from 0.5 to 1.0 g/g. When 1.0 g of catalyst per 1 g of xylose is used, about 87% and 65% of xylose are degraded by CS-CBSC and LR-CBSC, respectively. With a catalyst loading less than 0.5 g/g, the catalytical decomposition by CS-CBSC and SB-CBSC is almost the same with ~ 45–46%. Increasing the catalyst loading to over 0.5 g/g, CS-CBSC causes a stronger xylose decomposition than SB-CBSC does. In comparison with control sample, i.e., no solid acid catalyst was used, the xylose conversion efficiency was 14.05%, and the xylose conversion rate is significantly improved.

In general, there is no connection between the catalyst properties and xylose conversion activity since the catalyst structure and composition are quite complicated. It was reported that sulfonated carbon-based solid catalysts mainly contained three acidic groups (–SO_3H, –COOH, and phenol-OH). The synergistic action of those functional groups helped in enhancing the catalytic performance compared to conventional solid acids with single functional group –SO_3H (mainly) and -COOH acted as a Brønsted acid (Lin et al. 2019). This suggests that CS-CBSC and LR-CBSC

possess more -SO_3H groups than WS-CBSC does, which is also in compliance with TPD-NH_3 data shown earlier.

In all cases, 5-HMF is not detected in the condensed furfural nor in the residual reaction mixture. Under the applied conditions, the conversion of glucose to furfural is unlikely. Instead, there is a high possibility that glucose is decomposed totally or converted to HMF. However, the HMF formed is immediately degraded to humins or carboxylic acids, for example, formic, lactic, or levulinic acid as solid acid catalysts do not support the HMF-to-furfural conversion.

Influences of catalyst loading on furfural yield

Overall, the furfural yield descends with increasing catalyst dosages (Fig. 6). This is easily and clearly observed in the case of CS-CBSC. The amount of furfural formed rapidly decreases from its highest value of 28.6 to 2.3% when the catalyst loading of CS-CBSC increased from 0.1 to 1.0 g/g. Side-reactions were assumed to cause the loss of the final yield of furfural as summarized and discussed by Danon et al (2014). As mentioned in their review, furfural was possibly degraded to insoluble resinous products and other unidentified products. In addition, side-reactions between furfural and aldehydes could lead to the formation of humic substances. The other two CBSCs provide the highest yield of furfural at the dose of 0.2 g/g with 20.4% and 14.3% for WS-CBSC and LR-CBSC, respectively. The amount of furfural is also reduced rapidly at higher catalyst loading. The fast reduction in furfural yield when CS-CBSC was used suggests that this catalyst has strong catalytic activity and can be applied effectively to the production of furfural. The furfural yield remains stable at around 7–8% corresponding to the SB-CBSC loading of 0.1–0.5 g/g. However, like other catalysts, with increasing amount this catalyst also causes furfural decomposition. When conducting the reaction without using catalyst, the furfural yield was 4.03%. Surprisingly, when using WS- and CS-CBSC at

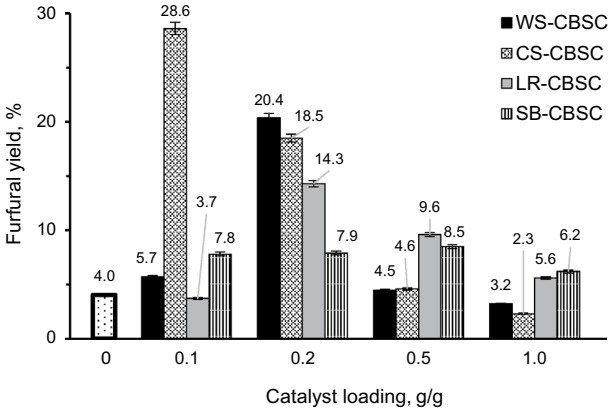

Fig. 6 Influence of catalyst loading on furfural yield; reaction conditions: temperature 150 °C, time 7 h (*WS Acacia mangium* wood sawdust, *LR* lignin-rich residue, *CS* coconut shell, *SB* sugarcane bagasse, *CBSC* carbonaceous sulfonated solid acid catalyst)

the dose of 1.0 g/g, the amount of furfural formed is even lower than without catalyst. This suggests that WS- and CS-CBSCs have stronger effect on the degradation of furfural than the other catalysts.

In conclusion, suitable catalyst doses for the synthesis of furfural are 0.1 g/g for CS-CBSC and SB-CBSC; 0.2 g/g for WS-CBSC and LR-CBSC. In all cases, the addition of the solid catalysts improves the reactions of xylose dehydration to furfural, which increases the furfural yield by about 3.5–7 times higher in comparison with control sample, i.e., no solid acid catalyst was used (the furfural yield was 4.05%).

Influences of catalyst loading on furfural selectivity

According to Fig. 7, at a suitable catalyst dose (i.e., 0.2 g/g) as mentioned earlier, WS-CBSC and LR-CBSC provided the highest furfural selectivity with 59.8 and 70.8%, respectively. When CS-CBSC and SB-CBSC are used, the selectivity of furfural is 40.8 and 15.6%, respectively. CS-CBSC seems to show better selectivity with 63.7% when it was used at a loading of 0.1 g/g. Considering both furfural selectivity and catalyst dosage, CS-CBSC is better than the other three catalysts. This is reasonable as CS-CBSC also provides the highest furfural yield of 28.6% at 0.1 g/g loading as mentioned earlier.

In comparison with the control sample, it can be seen that the effect of the catalyst used on the conversion of xylose to furfural is different. In most of the cases, the use of CBSCs significantly improves the selectivity. At a catalyst loading of 0.1 g/g, CS-CBSC provides the highest selectivity of 63.7%. When using 0.2 g/g of the catalyst, the best selectivity of 70.8% is reached in the case of using LR-CBSC. However, SB-CBSC does not show any enhancement as it gives lower selectivity than the control sample at all of the catalyst loadings.

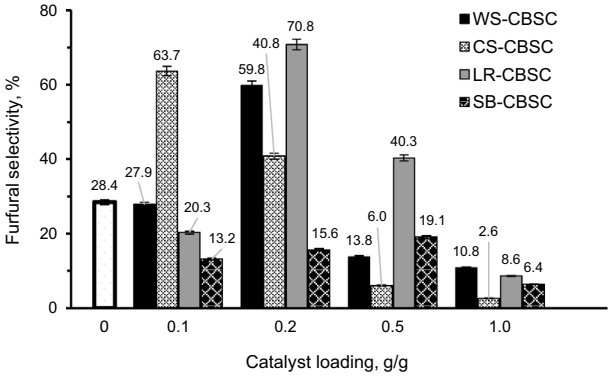

Fig. 7 Influence of catalyst loading on furfural selectivity; reaction conditions: temperature 150 °C, time 7 h (*WS* Acacia mangium wood sawdust, *LR* lignin-rich residue, *CS* coconut shell, *SB* sugarcane bagasse, *CBSC* carbonaceous sulfonated solid acid catalyst)

In conclusion, under suitable conditions (i.e., 0.1 g/g of catalyst loading), the highest furfural yield of 28.6%, 20.4%, 14.3%, and 7.9% can be achieved when using CS-, WS-, LR-, and SB-CBSC, respectively. Compared to other catalysts, which are more expensive (Zhang et al. 2017), the yield of furfural obtained in this work is equivalent or higher than when using montmorillonite K-10, $H_3O_{40}PWP_{12}$, SAPO-5, SAPO-11, metal modified beta zeolites (Al-Beta, Fe-Beta, Cr-Beta) for the synthesis of furfural from D-xylose at 175 °C or from corncob and sugarcane bagasse at 184 °C.

Conclusion

Sulfonated carbon-based solid acid catalysts are successfully synthesized from four sources of lignocellulosic biomass and applied to the production of furfural. The raw materials are activated with phosphoric acid for later development of porosity of the carbonized biochar. The sulfonation conducted at a low temperature for a long period of time allows good distribution of functional groups on the surface of the CBSCs. The CBSCs produced from the lignocellulosic refineries have acidity ranging from 4.5 to 7.2 mmol/g. Among the four sources, WS and LR provided the catalysts with higher surface areas than CS and SB. Regarding the conversion of the acidic hydrolysate, which mainly contains xylose, to furfural at 150 °C, the highest furfural yield of 28.6% is achieved when 10 wt% of CS-CBSC over xylose was used. However, at higher catalyst dosages (i.e., 20 wt%), WS-CBSC results in the greatest percentage of furfural formed with 20.4%.

Lignocellulosic materials with high content of lignin result in CBSCs with high total acidity, and therefore, xylose conversion is also higher with increasing catalyst dosage. Too much CBSC used (greater than 0.2 g/g) decreases the yield and selectivity of furfural. This finding significantly contributes to the completion of CBSCs production and application to the dehydration of carbohydrates.

Acknowledgements The authors would like to thank the Vietnam National Foundation for Science and Technology Development (NAFOSTED) for financially supporting this work under Grant No. 104.01-2017.304.

Funding This work was supported by the Vietnam National Foundation for Science and Technology Development (NAFOSTED) under Grant No. 104.01–2017.304.

Declarations

Conflicts of interest All the authors declare that they have no conflict of interests.

References

Bayu A, Abudula A, Guan G (2019) Reaction pathways and selectivity in chemo-catalytic conversion of biomass-derived carbohydrates to high-value chemicals: a review. Fuel Process Technol 196:106–162. https://doi.org/10.1016/j.fuproc.2019.106162

Bhaumik P, Dhepe PL (2016) Solid acid catalyzed synthesis of furans from carbohydrates. Catal Rev Sci Eng 58:36–112. https://doi.org/10.1080/01614940.2015.1099894

Chen G, Fang B (2011) Preparation of solid acid catalyst from glucose-starch mixture for biodiesel production. Bioresour Technol 102:2635–2640. https://doi.org/10.1016/j.biortech.2010.10.099

Chung NH, Phuong NTM, Dien LQ, Khanh NV (2019) Saccharification of Acacia mangium wood sawdust with dilute sulfuric acid for furfural production. Vietnam J Chem 57:753–757. https://doi.org/10.1002/vjch.2019000117

Danon B, Marcotullio G, De Jong W (2014) Mechanistic and kinetic aspects of pentose dehydration toward furfural in aqueous media employing homogeneous catalysis. Green Chem 16:39–54. https://doi.org/10.1039/c3gc41351a

De S, Dutta S, Saha B (2016) Critical design of heterogeneous catalysts for biomass valorization: current thrust and emerging prospects. Catal Sci Technol 6:7364–7385. https://doi.org/10.1039/c6cy01370h

Delbecq F, Wang Y, Muralidhara A, El Ouardi KE, Marlair G, Len C (2018) Hydrolysis of hemicellulose and derivatives-a review of recent advances in the production of furfural. Front Chem. https://doi.org/10.3389/fchem.2018.00146

Endut A, Abdullah SHYS, Hanapi NHM, Hamid SHA, Lananan F, Kamarudin MKA, Umar R, Juahir H, Khatoon H (2017) Optimization of biodiesel production by solid acid catalyst derived from coconut shell via response surface methodology. Int Biodeterior Biodegrad 124:250–257. https://doi.org/10.1016/j.ibiod.2017.06.008

Freitas JV, Nogueira FGE, Farinas CS (2019) Coconut shell activated carbon as an alternative adsorbent of inhibitors from lignocellulosic biomass pretreatment. Ind Crops Prod 137:16–23. https://doi.org/10.1016/j.indcrop.2019.05.018

Ghysels S, Ronsse F, Dickinson D, Prins W (2019b) Production and characterization of slow pyrolysis biochar from lignin-rich digested stillage from lignocellulosic ethanol production. Biomass Bioenerg 122:349–360. https://doi.org/10.1016/j.biombioe.2019.01.040

Ghysels S, Estrada Léon AE, Pala M, Schoder KA, Van Acker J, Ronsse F (2019a) Fast pyrolysis of mannan-rich ivory nut (Phytelephas aequatorialis) to valuable biorefinery products. Chem Eng J 373:446–457. https://doi.org/10.1016/j.cej.2019.05.042

Ghysels S, Acosta N, Estrada A, Pala M, De Vrieze J, Ronsse F, Rabaey K (2020) Integrating anaerobic digestion and slow pyrolysis improves the product portfolio of a cocoa waste biorefinery. Sustain Energy Fuels 4:3712–3725. https://doi.org/10.1039/d0se00689k

Gromov NV, Taran OP, Parmon VN (2018) Chapter 3: catalysts for depolymerization of biomass. In: RSC green chemistry. Royal society of chemistry, pp 65–97

Hara M, Nakajima K, Kamata K (2015) Recent progress in the development of solid catalysts for biomass conversion into high value-added chemicals. Sci Technol Adv Mater 16:1–22. https://doi.org/10.1088/1468-6996/16/3/034903

Hu L, Zhao G, Tang X, Wu Z, Xu J, Lin L, Liu S (2013) Catalytic conversion of carbohydrates into 5-hydroxymethylfurfural over cellulose-derived carbonaceous catalyst in ionic liquid. Bioresour Technol 148:501–507. https://doi.org/10.1016/j.biortech.2013.09.016

Hu L, Tang X, Wu Z, Lin L, Xu J, Xu N, Dai B (2015) Magnetic lignin-derived carbonaceous catalyst for the dehydration of fructose into 5-hydroxymethylfurfural in dimethylsulfoxide. Chem Eng J 263:299–308. https://doi.org/10.1016/j.cej.2014.11.044

Kang S, Ye J, Chang J (2013b) Recent advances in carbon-based sulfonated catalyst: preparation and application. Int Rev Chem Eng 5:133–144. https://doi.org/10.15866/ireche.v5i2.6912

Kang S, Ye J, Zhang Y, Chang J (2013a) Preparation of biomass hydrochar derived sulfonated catalysts and their catalytic effects for 5-hydroxymethylfurfural production. RSC Adv 3:7360–7366. https://doi.org/10.1039/c3ra23314f

Li H, Deng A, Ren J, Liu C, Lu Q, Zhong L, Peng F, Sun R (2014) Catalytic hydrothermal pretreatment of corncob into xylose and furfural via solid acid catalyst. Bioresour Technol 158:313–320. https://doi.org/10.1016/j.biortech.2014.02.059

Li X, Jia P, Wang T (2016) Furfural: a promising platform compound for sustainable production of C4 and C5 chemicals. ACS Catal 6:7621–7640. https://doi.org/10.1021/acscatal.6b01838

Li W, Zhu Y, Lu Y, Liu Q, Guan S, Chang H, Jameel H, Ma L (2017) Enhanced furfural production from raw corn stover employing a novel heterogeneous acid catalyst. Bioresour Technol 245:258–265. https://doi.org/10.1016/j.biortech.2017.08.077

Lin Q, Zhang C, Wang X, Cheng B, Mai N, Ren J (2019) Impact of activation on properties of carbon-based solid acid catalysts for the hydrothermal conversion of xylose and hemicelluloses. Catal Today 319:31–40. https://doi.org/10.1016/j.cattod.2018.03.070

Liu WJ, Tian K, Jiang H, Yu H-Q (2013b) Facile synthesis of highly efficient and recyclable magnetic solid acid from biomass waste. Sci Rep 3:2419. https://doi.org/10.1038/srep02419

Liu T, Li Z, Li W, Shi C, Wang Y (2013a) Preparation and characterization of biomass carbon-based solid acid catalyst for the esterification of oleic acid with methanol. Bioresour Technol 133:618–621. https://doi.org/10.1016/j.biortech.2013.01.163

Liu WJ, Jiang H, Yu HQ (2015) Development of Biochar-Based Functional Materials: Toward a Sustainable Platform Carbon Material. Chem Rev 115:12251–12285

Luo Y, Li Z, Li X, Liu X, Fan J, Clark JH, Hu C (2019) The production of furfural directly from hemicellulose in lignocellulosic biomass: A review. Catal Today 319:14–24. https://doi.org/10.1016/j.cattod.2018.06.042

Mamman AS, Lee JM, Kim YC, Hwang IT, Park NJ, Hwang YK, Chang JS, Hwang JS (2008) Furfural: Hemicellulose/xylose-derived biochemical. Biofuels Bioprod Biorefining 2:438–454

Marikutsa A, Sukhanova A, Rumyantseva M, Gaskov A (2018) Acidic and catalytic co-functionalization for tuning the sensitivity of sulfated tin oxide modified by ruthenium oxide to ammonia gas. Sens Actuators B Chem 255:3523–3532. https://doi.org/10.1016/j.snb.2017.09.186

Mariscal R, Maireles-Torres P, Ojeda M, Sádaba I, López Granados M (2016) Furfural: a renewable and versatile platform molecule for the synthesis of chemicals and fuels. Energy Environ Sci 9:1144–1189. https://doi.org/10.1039/c5ee02666k

Metkar PS, Till EJ, Corbin DR, Pereira CJ, Hutchenson KW, Sengupta SK (2015) Reactive distillation process for the production of furfural using solid acid catalysts. Green Chem 17:1453–1466. https://doi.org/10.1039/c4gc01912a

Pituya P, Sriburi T, Wijitkosum S (2017) Properties of biochar prepared from acacia wood and coconut shell for soil amendment. Eng J 21:63–76. https://doi.org/10.4186/ej.2017.21.3.63

SDG (2019) Sustainable Development Knowledge Platform. https://sustainabledevelopment.un.org/sdgs. Accessed 17 Apr 2020

Suganuma S, Nakajima K, Kitano M, Yamaguchi D, Kato H, Hayashi S, Hara M (2008) Hydrolysis of cellulose by amorphous carbon bearing SO3H, COOH, and OH groups. J Am Chem Soc 130:12787–12793. https://doi.org/10.1021/ja803983h

Thanh NT, Long NH, Dien LQ, Phuong Ly GT, Hoang PH, Minh Phuong NT, Hue NT (2019) Preparation of carbonaceous solid acid catalyst from Acacia mangium wood sawdust for conversion of same source into 5-hydroxymethylfurfural. Energy Sources Part A Recover Util Environ Eff 42:730–739. https://doi.org/10.1080/15567036.2019.1602195

Tomczyk A, Sokołowska Z, Boguta P (2020) Biochar physicochemical properties: pyrolysis temperature and feedstock kind effects. Rev Environ Sci Biotechnol 19:191–215

VPPA (2019) Vietnam - The world's largest exporter of wood chips and its impact on the pulp market. https://www.paper-vietnam.com/en/news/vietnam-the-worlds-largest-exporter-of-wood-chips-and-its-impact-on-the-pulp-market-2-99.html. Accessed 17 Apr 2020

Wang J, Xu W, Ren J, Liu X, Lu G, Wang Y (2011) Efficient catalytic conversion of fructose into hydroxymethylfurfural by a novel carbon-based solid acid. Green Chem 13:2678–2681. https://doi.org/10.1039/c1gc15306d

Zhang H, Liu X, Lu M, Hu X, Lu L, Tian X, Ji J (2014) Role of Brønsted acid in selective production of furfural in biomass pyrolysis. Bioresour Technol 169:800–803. https://doi.org/10.1016/j.biortech.2014.07.053

Zhang L, Xi G, Yu K, Yu H, Wang X (2017) Furfural production from biomass–derived carbohydrates and lignocellulosic residues via heterogeneous acid catalysts. Ind Crops Prod 98:68–75. https://doi.org/10.1016/j.indcrop.2017.01.014

Zhu J, Gan L, Li B, Yang X (2017) Synthesis and characteristics of lignin-derived solid acid catalysts for microcrystalline cellulose hydrolysis. Korean J Chem Eng 34:110–117. https://doi.org/10.1007/s11814-016-0220-5

Zhu Y, Li Z, Chen J (2019) Applications of lignin-derived catalysts for green synthesis. Green Energy Environ 4:210–244

Žilnik LF, Grilc V, Mirt I, Cerovečki Ž (2016) Study of the influence of key process parameters on furfural production. Acta Chim Slov 63:298–308. https://doi.org/10.17344/acsi.2016.2232